SSRG International Journal of Electrical and Electronics Engineering
ISSN: 2348-8379/ https://doi.org/10.14445/23488379/IJEEE-V11I5P124

Volume 11 Issue 5, 268-276, May 2024


*Original Article*

# Optimizing 400kV Bus Bar Performance for Enhanced Reliability and Voltage Dip Reduction

Ahmed A. Mohsen[1], Firas Mohammed Tuaimah[2], Yasser F. Gazi[3]

[1,3]*Department of Electrical and Electronic, University of Karbala, Karbala, Iraq.*
[2] *Department of Electrical, University of Baghdad, Baghdad, Iraq.*

[1]*Corresponding Author : Ahmed.mohsen@s.uokerbala.edu.iq*

Received: 14 March 2024 Revised: 15 April 2024 Accepted: 12 May 2024 Published: 29 May 2024

***Abstract*** *- The electrical grid in Iraq is dealing with increased demand due to expansion and climate change effects, notably at the 400 KV voltage level. This has led to lower bus bar voltages and reliability issues. To understand these challenges, a research study was conducted using the PSSE and ETAP software to analyze network reliability, including fault frequencies and failure rates across various timeframes. In the SMWCC/24401 area of the southern city, solar panels were used to link the bus rails. The research aimed at enhancing the bus bars' dependability, calculating the System Average Interruption Frequency Index (SAIFI) and System Average Interruption Duration Index (SAIDI) for three voltage scenarios, and assessing the Expected Energy Not Supplied (EENS) for each scenario based on voltage and power line connection changes Index Terms Photovoltaic (PV) power systems, Reliability of composite systems, Reliability modeling of PV systems.*

***Keywords*** *- Electrical grid, Reliability of power system, Photovoltaic cells, SAIFI and SAIDI, Electrical grid in Iraq.*

## 1. Introduction

Supply of electricity with minimal to no power that the system should provide a steady electricity supplier outages or interruptions [1]. The electrical system performs more effectively when dependability is guaranteed through the use of reliability evaluation methodologies. The utility and its customers suffer negative economic effects from interruption costs and power outages if this power is not planned for and kept reliable [2]. The development and prosperity of a nation are primarily impacted by the dependability and quality of its electrical supply, which is also closely linked to customer satisfaction [3]. Providing consumers with adequate and effective energy is the primary duty of the power system. Under typical circumstances, the power system must be extremely safe and efficient [4].

To satisfy the ever-increasing customer load requirements, power system planners work to find the best possible compromise between economics and reliability. Power system planners strive to determine the optimum balance between costs and reliability to meet the ever-increasing customer load requirements [5]. Among the most crucial elements in the design and operation of a power system is power system reliability. To guarantee the system operates dependably, system operators must obtain additional capacity due to the unplanned failures of generators. Conversely, the aimless growth of generators may result in significant societal expenses. Thus, to create suitable generation growth plans, reliability parameters must be established, and reliability must be expressed quantitatively [6].

## 2. Principles with Reliability Analyzation

Electrical reliability was divided into System security and adequacy [7]. Security has to do with the system's capacity to tolerate disturbances, whereas adequacy has to do with its ability to meet the demand. Power system security can be defined as the possibility that, given the likelihood of changes to the system and its surroundings, the system operating point will stay within allowable bounds [8].

### *2.1. Reliability Assessments*

According to [10], Reliability Assessments can be divided into two topologies:

Two-State Topology is shown in Figure 1.

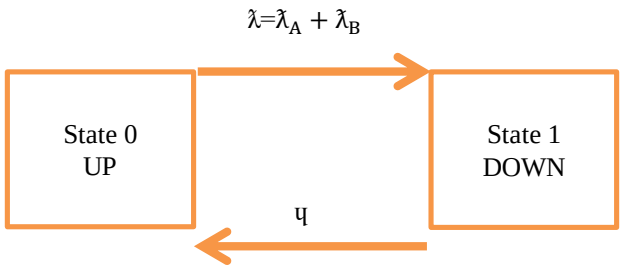


**Fig. 1 Tow state topology**

According to (Figure 1) state (0) indicates the normal operation of the power system. The state (1) indicate the disturbance (failed) mode, and (ƛ) amount of Changes occur.

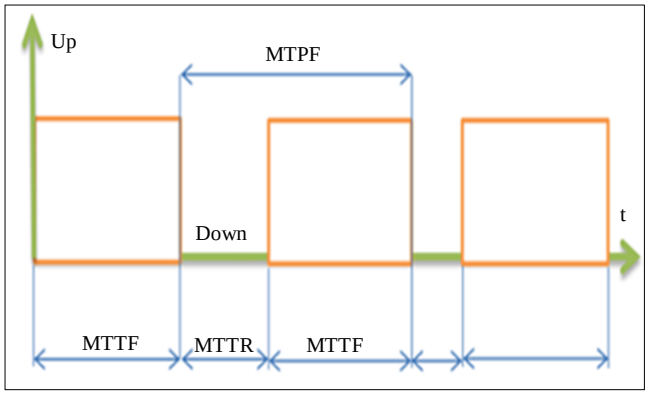


**Fig. 2 Two states that topology average time**

In the series Part, both (part 1 and part 2) must remain undamaged to ensure the regular operation of the system.

ƛ : Rate of frailer
$ƛ_A$ : Quick frailer
$ƛ_B$ : Pervious frailer
ɥ : Time absorbed
MTTF : Absorb time through fault
MTTR : Average time through Repair

$$MTBF: MTTF = 1/ ƛ \quad (1)$$

$$MTTR = 1/ ɥ \quad (2)$$

$$MTBF = ( MTTF + MTTR) \quad (3)$$

### *2.2. Two-Series Topology*

According to [12] Two-Series Topology divided into two types:

Series part, as shown in Figure 3.

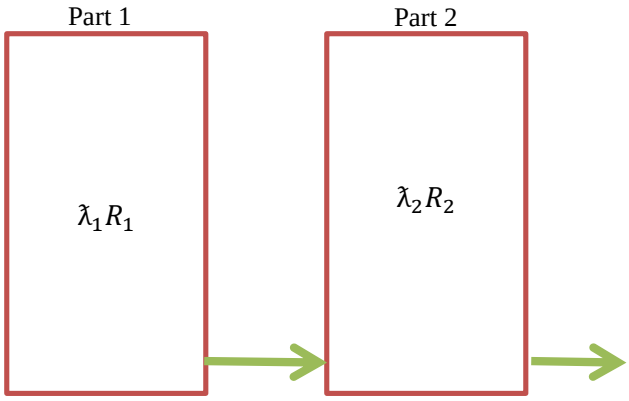


**Fig. 3 Series part**

$ƛ_n$ , $R_n$ Frailer rate and Repair time, respectively.

Parallel part as shown in Figure 4.

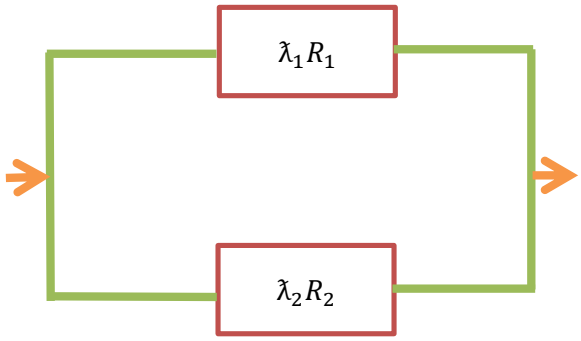


**Fig. 4 Parallel part**

$ƛ_n$ , $R_n$ Frailer rate and Repair time, respectively. When a system operates in parallel, the load failure modes entail multiple outages, meaning that two or more outages go down simultaneously.

## 3. Modeling Reliability of PV System Components

PV reliability evaluation serves two main purposes. Firstly, it assesses the performance of PV systems. Secondly, it produces reliability indices that are valuable in choosing the optimal design option and identifying operationally beneficial and cost-saving improvements. Two categories of reliability indices are presented to achieve these objectives: time-oriented indices and energy-oriented indices [13]. (Figure 5) displays strings attached to a DC combiner with an ignition switch and safety components.

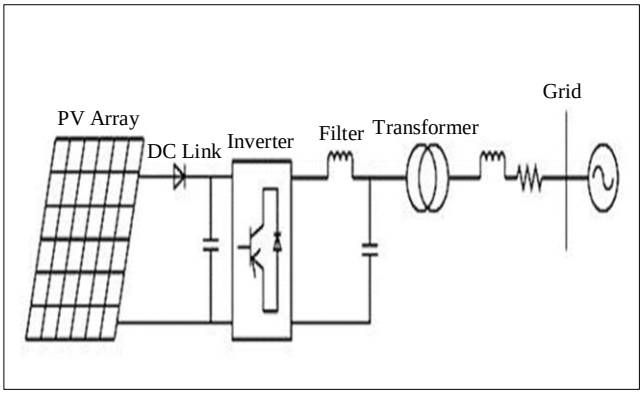


**Fig. 5 Schematic diagram of a PV power system using central inverters [20]**

This text describes an extensive photovoltaic system that is connected to the grid. The text examines the general image of the system while also delving into the specifics of PV reliability evaluation. The system consists of several PV arrays that make up the three-phase central inverter PV system, as seen in Figure 1. PV strings are linked to a DC

combiner, which contains fuses and additional safety components for each array. The DC power from the photovoltaic array passes through DC breaks, which, in the event of a failure, leave visible gaps and act to separate the arrays from the rest of the system. The utility system receives three-phase power from the central inverter, which supplies the full phase's worth of AC power, typically at 208 V, via an AC sub-panel to an AC disconnect or breaker. The dependability assessment of large-scale commercial PV systems is done in two steps [13].

## 4. Maintaining the Longevity and Reliability of Photovoltaic Systems

As the focus on environmentally friendly emissions and sustainability grows, traditional fossil fuel-based power generation is being phased out, and renewable energy sources are becoming increasingly prevalent. However, as the proportion of green energy in the overall energy mix increases, it becomes more challenging to ensure its reliability. Unlike conventional power sources, the output of Photovoltaic (PV) and Wind Turbines (WT) is heavily influenced by factors such as solar radiation and wind speed [14].

## 5. PV Generator System Evaluation [11, 14]

The PV derating factor is a factor that scales the output of a PV array to account for inefficiencies caused by higher temperatures, fluctuating operational voltages, and solar soiling. This factor is generally between 0 and 100 percent.

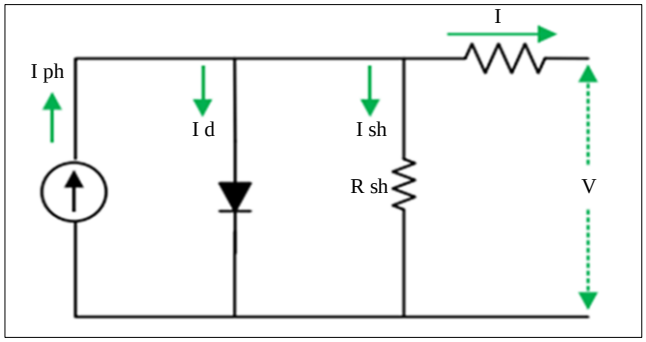


**Fig. 6 solar PV equivalent circuit**

The network in Figure 6 represents a real solar panel, and the Kirchhoff equation can be utilized to find the current at the output of the PV cell.

$$I = I_{ph} - (I_d + I_{sh}\ ) \tag{4}$$

$$I_{ph} = (I_{scr} + K_i \triangle_i)\frac{G}{Gr} \tag{5}$$

The photocurrent is represented by *Iph*, the current through the diode by *Id*, and the current leak in the form of a shunt resistor by *Ish*, which is often extremely small and can be disregarded. Iscr is a way to measure the electrical current produced by solar panels under certain conditions, typically with a temperature of 250°C.

Ki is a symbol used to represent the heating coefficient when there is a short circuit in the solar panel system.

G is the amount of sunlight that reaches a Photovoltaic (PV) cell, measured in watts per square meter (W/m²).

The "η ΔT" symbol refers to the difference in temperature between the PV cell when it is producing power and the reference temperature (Tref). The output current $I_O$:

$$I = I_{ph} - I_0 \tag{6}$$

## 6. The PV Device's Efficiency from [15]

The efficiency of a PA photovoltaic device is dependent on the distribution of the solar radiation spectrum. To evaluate the performance of PV devices, a standard spectral distribution is used as a reference. This is done to compare the performance of different PV cells using standardized parameters. The datasheet of a PV cell typically includes these parameters. The datasheets provide impressive information about the performance and characteristics of PV arrays under common test conditions. The standard test conditions are referred to as nominal or standard test circumstances and are conducted using a V apparatus [15]. The test conditions are as follows:

$$I_{irradiance}(G_n) = 1000\frac{W}{m^2} \tag{7}$$

The distribution of the solar density will be = 1.5 A.M

## 7. DC Input Voltage of an Inverter

When selecting an inverter's Direct Current Voltage (VDC), it is important to consider the inverter output voltage. For single-phase transformer-less inverters, the necessary VDC can be determined using Equation (6), where Ma is an index of modulation and Vrms represents the inverter's output value. It is not recommended to select Ma to be more than 1, as this will increase the inverter's final voltage's Total Harmonic Distortion (THD). Therefore, for inverters that use Sine Pulse Width Modulation (SPWM) with DC input voltages, the minimum required VDC can be calculated by using Ma=1 in Equations (8), and (9) [16].

$$V_{rms} = \frac{V_{DC}\,x M_a}{\sqrt{2}} \tag{8}$$

$$V_{rms}(LL) = \sqrt{\frac{3}{2}}\ x\ \ \frac{V_{DC}}{2}\,x M_a \tag{9}$$

## 8. The Solar Power Array's Size

It is necessary to calculate the array's size, its direct current (VDC), the mean daily solar hours (Tmin

temperatures), and the entire every day in Watts of power (E). After these variables are accessible, the scaling procedure is initiated.

To avoid underestimating solar panel needs, we divide the total average energy demand per day by the efficiencies of the system components to determine the daily energy requirement from the solar array [17].

$$E_r = \frac{\text{daily energy consumption}}{\text{product of componente'efficiencies}} \quad (10)$$

The peak power equation will be

$$P_P = \frac{\text{The daily energy required}}{\text{minimum peak sun-our per day}} = \frac{E_r}{T_{min}} \quad (11)$$

The output DC current of the pav array will be calculated from Equation (12).

$$I_{DC} = \frac{P_P}{\text{System dc voltage}} = \frac{p_p}{V_{DC}} \quad (12)$$

## 9. Qty of Photovoltaic Modules

The standard testing parameters for commercial photovoltaic modules typically involve exposing them to 1000W/m2 of solar energy, with panel temperatures of 25ºC and 1.5 air mass. These tests are conducted to determine the specific power rating of the modules. In this study, sunlight is considered to be less than 1000W/m2, or 750W/m2, as long as it accounts for overcast days and is not consistently at 1000W/m2. To calculate the total number of PV modules, we need to follow a specific process [18].

$$N = \frac{P_t}{P_m} = \frac{P_t}{\eta_m G A_M} \quad (13)$$

The formula to calculate the total number of PV modules is n_r x n_m = N, where n_r is the number of rows and n_m is the number of photovoltaic cells in each row. To determine N, you need to know the size of each module (A_m) in square meters, the amount of incident sunlight in watts per square meter (G), the total installation power capacity in watts (P_t), and the module efficiency under typical test conditions (η_m).

$$N = n_r X n_m \quad (14)$$

## 10. Aim of this Paper

This paper aims to investigate the dependability of one of the 400 KV voltage bars in the southern region of Iraq, known as SMWCC/24401. These bars are known to experience voltage drops frequently. To reduce this issue, a solar renewable energy system has been connected. The paper will examine the load reliability when the load is connected to these bars after network improvement. It will also present a case study of the same load's reliability when fed by one or two power transmission lines. The study will then select one of the cases.

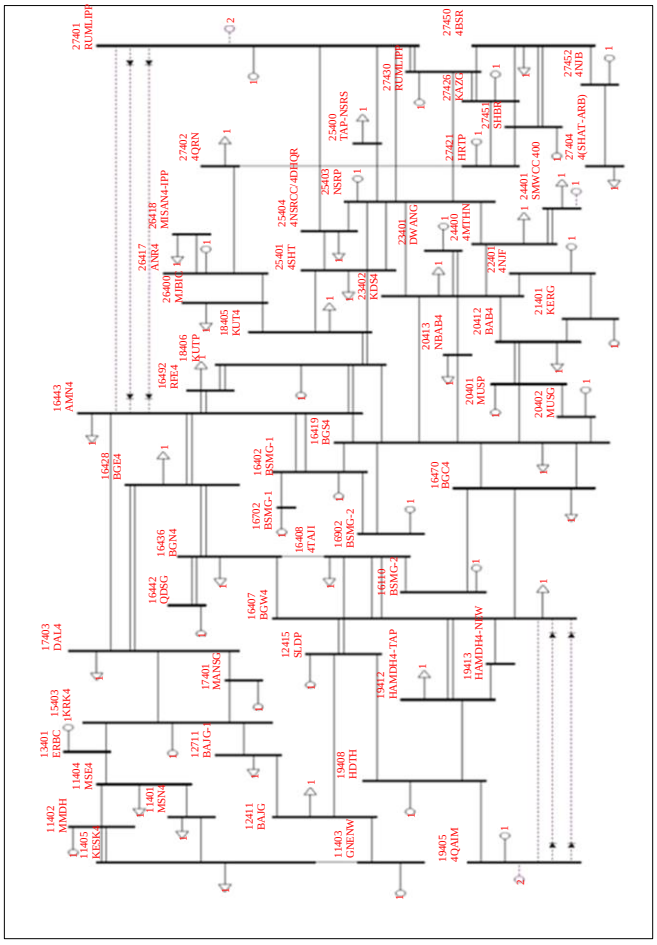

**Fig. 7 400KV super Iraqi grid-PSS/E software layout**

## 11. Density of Solar Radiance in Iraq

Iraq is known for having extended daylight hours, receiving over 3000 hours of sun radiation in Baghdad each year. The hourly solar intensity varies between 416 W/m2 in January and 833 W/m2 in June. In fact, Iraq has recorded more sunlight hours than any other country. However, despite having great potential, solar technologies are not widely used in the country.

Compared to other places, the western Iraqi desert has the highest solar irradiance for generating electric power. This is in contrast to the global average horizontal surface irradiance of 170 W/m2 per year. According to research by the German Aerospace Institute, Iraq's deserts generate power at an average of 270 to 290 W/m2, with a peak power density of 2310 kWh/m2/year. This translates to approximately 31 percent of the country's total land area [19].

## 12. Iraqi Super Grid 400KV.

From the perspective of the Iraqi Ministry of Electricity, the power supply in Iraq is divided into three operational parts.

These include the Kurdistan area network, which is different from the overall Iraqi network, and the North, Middle, and South regions. The Iraqi HVAC transmission system has kV and a frequency of 50 Hz [20] operates at a voltage transmission range of 132 kV to 400. Figure 7 represents the single-line diagram of the 400KVsuper Iraqi Grid.

## 13. Simulations

The failure rate and repair rate values at droop voltage for BUS-KV-400 and improved voltage for BUS-KV-380, as well as for improved voltage for BUS-KV-400 and droop voltage for BUS-KV-380, remain constant. This is because the time required to transition from a state of zero to a state of one is still the same. However, the values for failure rate and repair rate at BUS-KV-400 parallel load line and improved voltage are different from those at BUS-KV-380 (at droop voltage) due to the increasing short circuit caused by double contingency.

At BUS BAR NO.1, the time required to transition from a state of zero to a state of one is higher than the same time of BUS-KV-400 and improved voltage and BUS-KV-380 (at droop voltage). Figure 8, which represents a research case, we notice the value of the voltage drop on the bus bars SMWCC 24401 from the Iraqi network with a high voltage of 400 kV, where the actual read value was equal to 376 kV, which represents outside the permissible limit and is considered one of the factors that reduce the reliability of the consumer in the system.

Electrician, where the above bars were chosen, and reliability parameters were extracted, and then, in Figure 9, after the voltage of the above bars was improved to reach the voltage of 400.5 by means of renewable energy added to the bars, the above parameters were recalculated in two cases, the first when the power transmission line was a single line and the second when it was Power transmission line in the case of two parallel lines and the values or parameters according to Table 1.

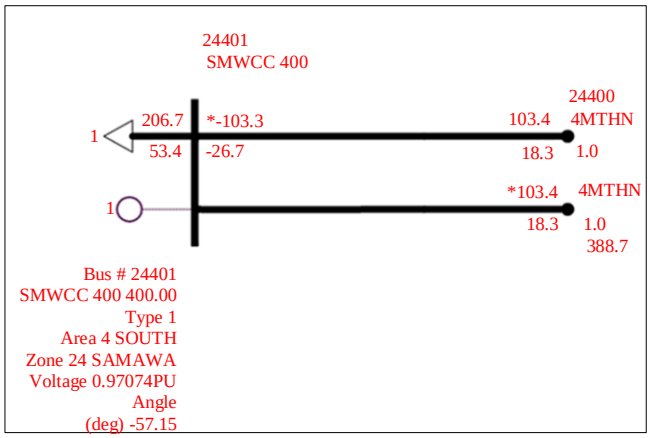


**Fig. 8 SMWCC bus bars are in a voltage drop state from the PSS/E layout**

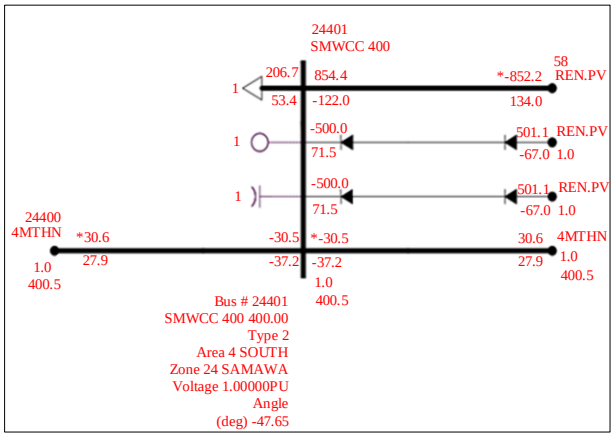


**Fig. 9 SMWCC bus bars after improved by PV array from PSS/E layout**

## 14. Results and Discussion

### *14.1. In Case of SMWCC Bus Bars are under Voltage Drop*

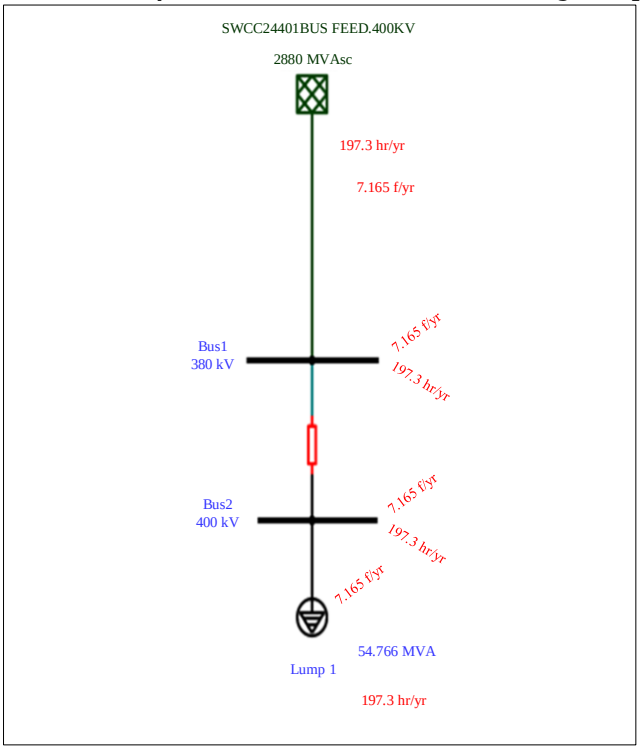


**Fig. 10 SMWCC bus bars reliability failure rate and repair rate from ETAP software layout at drop voltage**

From Figure 10, an analysis conducted by the ETAP software has revealed that bus bars numbered 1 have a failure rate of 7.166 per year. There is a probability of recurrence of the same fault on bus rails within a year, which is valued at 197.3 hours per year. The time required to repair faults on the tracks is measured in hours and for a year. It should be noted that the values mentioned above are in the case of a voltage drop for the SMWCC bars from the design voltage value of 400 KV to the drop value caused by excessive loads, which is down to 380 KV.

### *14.2. In the Case of SMWCC Bus Bars, Improvement is Achieved by Using a PV Array at One Transmission Line to Feed the load*

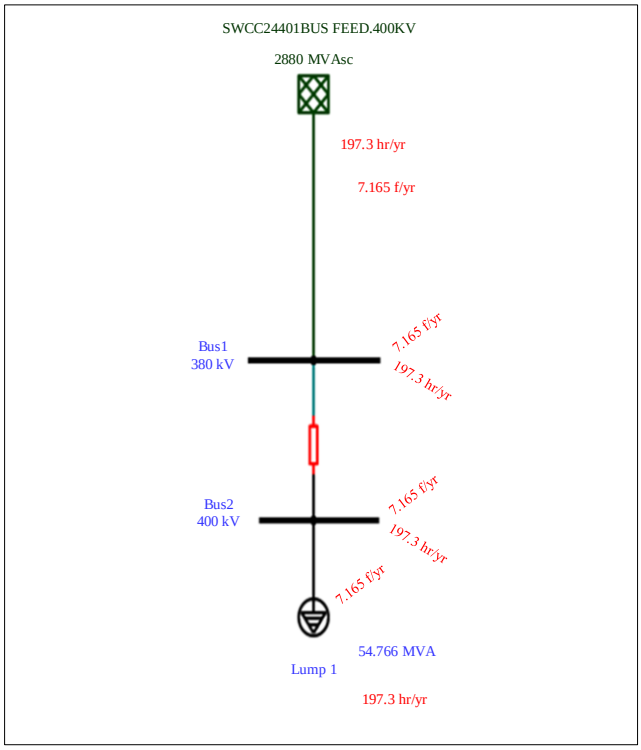


**Fig. 11 Reliability failure rate and repair rate for SMWCC bus bars obtained from ETAP software layout to reduce voltage drop on one transmission line fed load**

From Figure 11 according to the analysis conducted by the ETAP software, it has been found that the bus bars are numbered. According to an analysis conducted by the ETAP software, bus bars labeled 1 have a failure rate of 7.166 per year. There is a possibility of recurring faults on bus rails within a year, which amounts to 197.3 hours per year. The time required to repair faults on the tracks is measured in hours and for a year. Please note that these values are applicable when the voltage drop for the SMWCC bars is reduced by using the PV array and the SMWCC bus bars reach their normal operating bus voltage, which is 400 KV.

### *14.3. In the Case of SMWCC Bus Bars, Improvement is Achieved by Using a PV Array at the Tow Transmission Line to Feed the Load*

In Figure 12, a solar energy cell system was connected to a certain amount in order to reduce voltage drop and restore the normal voltage of 400 KV. A new power transmission line was added parallel to the old line to reduce losses while ensuring that the load continues to be equipped with electrical power. This increases the reliability of the customer's load in the event of a fault in one of them. The addition of the second line also helps to reduce the value of the Expected Energy Not Supplied (EENS) rate, as we notice that the value of the failure rate has decreased to 3.74 f/yr and the value of the Ribar rate has decreased to 62.7 hr/yr, meaning that the system has become much more reliable than before.

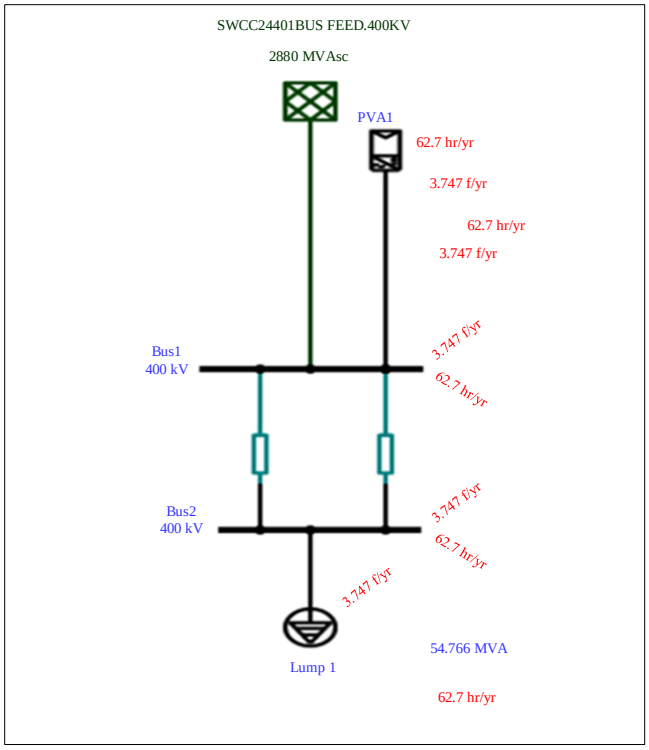


**Fig. 12 SMWCC BUS BARS reliability failure rate and repair rate from ETAP software layout**

### *14.4. Reliability Parameter*

Reliability consists of eight parameters, which are clearly defined below:

1. Average Customer Curtailment Index (ACCI) System
2. Average Energy Not Supplied (AENS)
3. ALII System - Average Connected kVA Interrupted per kVA of Connected Load Served
4. Average Service Availability Index (ASAI)
5. Average Service Unavailability Index (ASUI)
6. Customer Average Interruption Duration Index (CAIDI)
7. Customer Total Average Interruption Duration Index (CTAIDI) System
8. ECOST Expected Interruption Cost (ECOST)
9. EENS Expected Energy Not Supplied (EENS)
10. IEAR Interruption Energy Assessment Rate (IEAR)
11. Average Interruption Duration Index (ASIDI) System
12. Average Interruption Frequency Index (SAIFI) System

The failure rate and repair rate values at droop voltage for BUS-KV-400 and improved voltage for BUS-KV-380, as well as for improved voltage for BUS-KV-400 and droop voltage for BUS-KV-380, remain constant. This is because the time required to transition from a state of zero to a state of one is still the same. However, the values for failure rate and repair

rate at BUS-KV-400 parallel load line and improved voltage are different from those at BUS-KV-380 (at drop voltage) due to the increasing short circuit caused by double contingency.

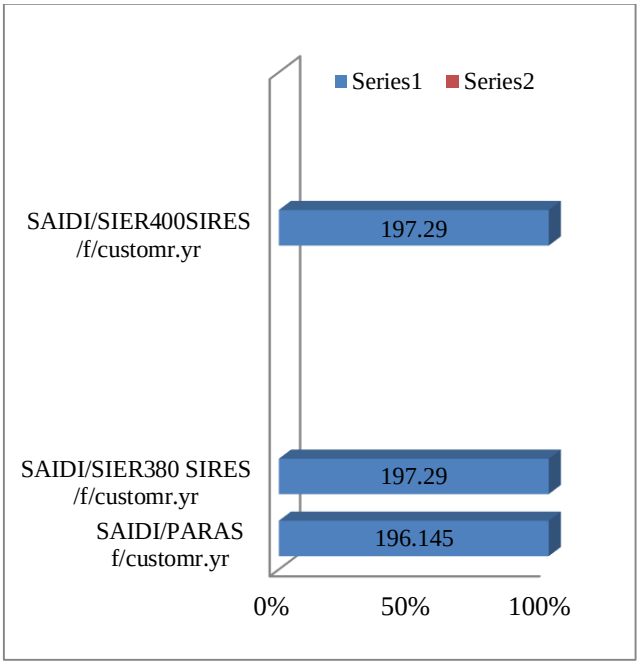


**Fig. 13 SAIDI worth for different types of load**

At BUS BAR NO.1, the time required to transition from a state of zero to a state of one is higher than the same time of BUS-KV-400 and improved voltage and BUS-KV-380 (at drop voltage) 10.2. It is evident from Figures 13 and 14 that the SAIF value for the customer. yr is much lower when compared to the SAID value for the same.

This is particularly true when the connection is meant to carry two parallel power transmission lines and when both SAIFI and SAIDI values are small. In such cases, the electrical system is considered to be more reliable.

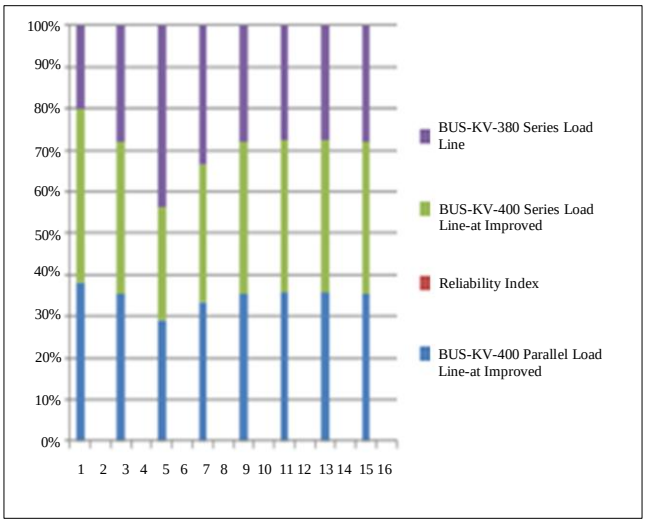


**Fig. 14 SAIDI worth for different types of load**

In the second scenario, a system improvement was made by adding solar system cells and connecting a new power transmission line. The ETAP program was used to extract the results, which indicated that the failure rate was 3.74 hours per year and the repair rate was 62.7 hours per year. As shown in Figures 12, 13, 14 and Table 1, these values are better than the previous ones because they are low. Therefore, improving any bus bars that suffer from voltage drops by using renewable energy to return them to nominal design voltages will result in stabilized bars and increased reliability.

**Table 1. Reliability parameter values**

| BUS –KV-400- Parallel Load Line at Improved | BUS –KV-400- Series Load Line at Improved | BUS –KV-380- Series Load Line at Drop Voltage | Reliability Index |
|---|---|---|---|
| 13.6650 | 7.1650 | 7.1650 | SAIFI f/customr.yr |
| 392.2900 | 197.2900 | 197.2900 | SAIDI f/customr.yr |
| 28.708 | 27.535 | 27.535 | CAIDI hr/customer.yr |
| 0.9552 | 0.9775 | 0.9775 | ASAI pu |
| 0.04478 | 0.02252 | 0.02252 | ASUI pu |
| 9332.8410 | 4693.661 | 4693.661 | EENS MW hr/.yr |
| 9332.8410 | 4693.661 | 4693.661 | AENS/MW hr/customer.yr |
| 0.04478 | 0.02252 | 0.02252 | ASUI PU. |

## 15. Conclusion

In order to thoroughly examine the conclusion over a certain period, we will make use of the information and statistics provided in Table 1, as well as the findings depicted in Figures 12, 13, and 14. This comprehensive analysis will enable us to gain a deeper understanding of the conclusion's evolution and any significant changes that may have occurred during that time.

1. At power system BUS –KV-400- Series load line-at improved the value of SAIFI (f/customr.yr) = 7.1650.
2. At power system BUS –KV-380- Series load line-at drop voltage the value of SAIFI (f/customr.yr) = 7.1650
3. AT POWER SYSTEM BUS –KV-400- parallel load line-at improved the value of SAIFI (f/customr.yr) = (13.66/2) = 6.83
   The system connected in parallel is more reliable based on the three values because having a low SAIFI value indicates good reliability.
4. At power system BUS –KV-400- Series load line-at improved the value of SAIDI (f/customr.yr) = 197.2900
5. At power system BUS –KV-380- Series load line- at drop voltage, the value of SAIDI (f/customr.yr) = 197.2900.
6. AT POWER SYSTEM BUS –KV-400- parallel load line-at improved the value of SAIDI (f/customr.yr) = (392.2900/2) = 196.145
   The system connected in parallel is more reliable based on the three values because having a low SAIDI value indicates good reliability.
7. At power system BUS –KV-400- Series load line-at improved the value of EENS (MW hr/.yr) = 4693.661.
8. At power system BUS –KV-380- Series load line- at drop voltage, the value of EENS (MW hr/.yr )) = 4693.661.
9. AT POWER SYSTEM BUS –KV-400- parallel load line-at improved the value of EENS (MW hr/.yr) = (9332.8410/2) = 4666.4205.

The system connected in parallel is more reliable based on the three values, because having a low EENS (MW hr/.yr). The EENS (MW hr/.yr) value represents the amount of money that is spent during the interruption.

## Acknowledgement

I want to dedicate this research to the professors who provided me with essential information to complete this work. Specifically, I would like to acknowledge Dr. Firas Muhammad, head of the Electricity Department at the University of Baghdad, and Dr. Yasser Falah, a professor at the University of Karbala, Department of Electrical and Electronic Engineering.

## References

[1] Abrha Hiluf, and Teshomen Goa Tella, "Reliability Assessment of Electrical Distribution Network using Analytical Method : A Case Study of Maychew City Distribution System," *International Journal of Engineering Research & Technology*, vol. 9, no. 8, pp. 977-985, 2020. [CrossRef] [Google Scholar] [Publisher Link]

[2] S. B. Aruna et al., "A Comprehensive Review on the Modern Power System Reliability Assessment," *International Journal of Renewable Energy Research*, vol. 11, no. 4, pp. 1734-1747, 2021. [CrossRef] [Google Scholar] [Publisher Link]

[3] Prakash Kafle, Manila Bhandari, and Lalit B. Rana, "Reliability Analysis Techniques in Distribution System: A Comprehensive Review," *International Journal of Engineering and Manufacturing*, vol. 12, no. 2, pp. 11-24, 2022. [CrossRef] [Google Scholar] [Publisher Link]

[4] Fengli Wang et al., "Reliability Evaluation of Substations Subject to Protection System Failures," *2013 IEEE Grenoble Conference*, France, pp. 1-6, 2013. [CrossRef] [Google Scholar] [Publisher Link]

[5] Sean Ericson, and Lars Lisell, "A Flexible Framework for Modeling Customer Damage Functions for Power Outages," *Energy Systems*, vol. 11, pp. 95-111, 2020. [CrossRef] [Google Scholar] [Publisher Link]

[6] Hyobin Oh et al., "Power System Reliability Evaluation Based on Chronological Booth-Baleriaux Method," *Applied Sciences*, vol. 13, no. 14, pp. 1-13, 2023. [CrossRef] [Google Scholar] [Publisher Link]

[7] Shoki Kosai, Chia Kwang Tan, and Eiji Yamasue, "Evaluating Power Reliability Dedicated for Sudden Disruptions: its Application to Determine Capacity on the Basis of Energy Security," *Sustainability*, vol. 10, no. 6, pp. 1-18, 2018. [CrossRef] [Google Scholar] [Publisher Link]

[8] Zhigang Lu et al., "A Security Level Classification Method for Power Systems under N-1 Contingency," *Energies*, vol. 10, no. 12, pp. 1-17, 2017. [CrossRef] [Google Scholar] [Publisher Link]

[9] Ramandip Singh, Jaspreet Singh, and Ramanpreet Singh, "Power System Security Using Contingency Analysis For Distributed Network," *International Journal of Engineering Research & Technology*, vol. 2, no. 4, pp. 1256-1261, 2013. [CrossRef] [Google Scholar] [Publisher Link]

[10] N. Adeyi, A. Akhikpemelo, and A. Eyibo, "Reliability Analysis of Power Distribution Network," *Continental Journal of Engineering Sciences*, vol. 11, no. 2, pp. 53-63, 2016. [Google Scholar]

[11] S. Sanajaoba Singh, and Eugene Fernandez, "Reliability Evaluation of a Solar Photovoltaic System with and without Battery Storage," *2015 Annual IEEE India Conference (INDICON)*, New Delhi, India, pp. 1-6, 2015. [CrossRef] [Google Scholar] [Publisher Link]

[12] Trygve Vesseltun Berg, "*Combining Analytical Power System Reliability Assessment Methods with Monte Carlo Simulation*," Master Thesis, Faculty of Information Technology and Electrical Engineering, Norwegian University of Science and Technology, 2019. [Google Scholar] [Publisher Link]

[13] Peng Zhang et al., "Reliability Evaluation of Grid-Connected Photovoltaic Power Systems," *IEEE Transactions on Sustainable Energy*, vol. 3, no. 3, pp. 379-389, 2012. [CrossRef] [Google Scholar] [Publisher Link]

[14] Muhammad Awais et al., "Comparative Assessment of Standalone Solar Photovoltaic Inverter Using Proteus and MATLAB Simulink Software," *European Journal of Science and Technology*, no. 30, pp. 6-11, 2021. [CrossRef] [Google Scholar] [Publisher Link]

[15] Marcelo Gradella Villalva, Jonas Rafael Gazoli, and Ernesto Ruppert Filho, "Modeling and Circuit-Based Simulation of Photovoltaic Arrays," *2009 Brazilian Power Electronics Conference*, Bonito-Mato Grosso do Sul, Brazil, pp. 1244-1254, 2009. [CrossRef] [Google Scholar] [Publisher Link]

[16] Moien A. Omar, and Marwan M. Mahmoud, "Improvement Approach for Matching PV-Array and Inverter of Grid Connected PV Systems Verified by a Case Study," *International Journal of Renewable Energy Development*, vol. 10, no. 4, pp. 687-697, 2021. [CrossRef] [Google Scholar] [Publisher Link]

[17] Ali Najah Al-Shamani et al., "Design & Sizing of Standalone Solar Power Systems a House Iraq," *Recent Advances in Renewable Energy Sources*, pp. 145-150, 2015. [Google Scholar]

[18] A. Al-Khazzar "The Required Land Area for Installing a Photovoltaic Power Plant," *Iranica Journal of Energy & Environment*, vol. 8, no. 1, pp. 11-17, 2017. [CrossRef] [Google Scholar] [Publisher Link]

[19] Hussain H. Al-Kayiem, and Sanan T. Mohammad, "Potential of Renewable Energy Resources with an Emphasis on Solar Power in Iraq: An Outlook," *Resources*, vol. 8, no. 1, pp. 1-20, 2019. [CrossRef] [Google Scholar] [Publisher Link]

[20] Israa Ismael Hussein, Sirine Essallah, and Adel Khedher, "Improvement of the Iraqi Super Grid Performance Using HVDC/HVAC Links by the Integration of Large-Scale Renewable Energy Sources," *Energies*, vol. 15, no. 3, pp. 1-19, 2022. [CrossRef] [Google Scholar] [Publisher Link]